RSC Advances

PAPER

View Article Online
View Journal | View Issue

Cite this: *RSC Adv.*, 2023, **13**, 3743

Improvements in piezoelectric and energy harvesting properties with a slight change in depolarization temperature in modified BNKT ceramics by a simple technique†

Pharatree Jaita,[abc] Kamonporn Saenkam[ad] and Gobwute Rujijanagul *[acef]

For many BNT-based ceramics, an attempt to increase the piezoelectric properties usually results in a decrease in depolarization temperature (T_d). This trend limits the applications of the materials. Many previous experiments have used different methods to enhance the piezoelectric properties and improve the T_d characteristic. In this study, we demonstrated a simple technique (thermal annealing) to enhance the piezoelectric properties with a very slight decrease in T_d by ~2 °C for a modified BNKT ceramic (BNKT doped with ZnO). Other phase transition characteristic temperatures of the studied ceramics were also slightly changed. The optimum dielectric ($\varepsilon_r = 651$, $\tan\delta = 0.0503$, $T_{F-R} = 167.38$ °C, $T_m = 305.41$ °C, $\varepsilon_{max} = 5551$, $T_B = 367.15$ °C, $T_d = 155.98$ °C, and $\gamma = 1.43$), ferroelectric ($P_{max} = 41.28$ μC cm^{-2}, $P_r = 35.85$ μC cm^{-2}, $E_c = 42.60$ kV cm^{-1} and $R_{sq} = 1.42$), piezoelectric ($d_{33} = 198$ pC N^{-1}, $k_p = 0.598$, and $g_{33} = 34.35 \times 10^{-3}$ Vm N^{-1}), and energy harvesting (FoM = 6.80 pm^2 N^{-1}) were obtained for the 8 h annealed ceramic. Furthermore, higher energy harvesting properties (which were 32% higher than that of the unannealed ceramic) were obtained after employing this technique.

Received 29th November 2022
Accepted 12th January 2023

DOI: 10.1039/d2ra07587c

rsc.li/rsc-advances

1 Introduction

Piezoelectric materials have been extensively designed and applied in many industrial fields, for example in such items as sensors, micro-displacement devices, brakes, sensitive materials, and other components, due to their ability to cause a mutual conversion between mechanical and electrical energy.[1] The development of piezoelectric materials with high energy conversion efficiency is of decisive importance for the requirements of advanced energy harvesting (EH) devices toward miniaturization and integration.[2] Lead titanate zirconate (PZT) ceramics are the most widely used energy harvesting materials due to their excellent piezoelectric properties,[3] *i.e.*, high mechanical quality factor (Q_m), high piezoelectric constant (d_{33}), and large planar electromechanical coupling factor (k_p).[4] However, lead-based compounds pose a serious environmental threat, and, therefore, efforts have been made to look for cleaner alternatives.[1,3]

Recent reports have identified many possible lead-free candidates based on barium titanate ($BaTiO_3$, BT), potassium sodium niobates ($K_{0.5}Na_{0.5}NbO_3$, KNN), bismuth sodium titanates ($Bi_{0.5}Na_{0.5}TiO_3$, BNT), bismuth potassium titanates ($Bi_{0.5}K_{0.5}TiO_3$, BKT), and bismuth layered ferroelectrics.[2,5] Among them, BNT has been found to be a possible energy storage material due to its high spontaneous polarization (P_m) exceeding 40 μC cm^{-2}, which results from the hybridization of the Bi 6p and O 2p orbitals.[6] Nevertheless, a pure BNT ceramic is known to be to be sintered with difficulty, and it also has other issues, such as beginning polarized with just as much complication, not to mention its having a high coercive field (E_c), high conductivity, and poor temperature stability.[7] Therefore, there is an urgent need for researchers to approach to improve the performance of the BNT ceramic. Numerous approaches, such as the establishment of the morphotropic phase boundaries (MPB), acceptor/donor dopants, compositional tuning, and improvement of the fabrication process conditions, have been proposed for the property optimization of the BNT piezoelectric materials.[8] Besides BNT, bismuth sodium potassium titanate or $Bi_{0.5}(Na_{1-x}K_x)_{0.5}TiO_3$ (BNKT) lead-free piezoelectric ceramic is also a good candidate for the replacement of toxic lead compounds for energy harvesting applications. For the

[a]*Department of Physics and Materials Science, Faculty of Science, Chiang Mai University, Chiang Mai 50200, Thailand. E-mail: rujijanagul@yahoo.com*

[b]*Office of Research Administration, Chiang Mai University, Chiang Mai 50200, Thailand*

[c]*Materials Science Research Center, Faculty of Science, Chiang Mai University, Chiang Mai 50200, Thailand*

[d]*Graduate School, Chiang Mai University, Chiang Mai 50200, Thailand*

[e]*Science and Technology Research Institute, Chiang Mai University, Chiang Mai 50200, Thailand*

[f]*Research Center in Physics and Astronomy, Faculty of Science, Chiang Mai University, Chiang Mai 50200, Thailand*

† Electronic supplementary information (ESI) available. See DOI: https://doi.org/10.1039/d2ra07587c

$Bi_{0.5}(Na_{1-x}K_x)_{0.5}TiO_3$ solid solution, Na^+ is partially substituted by K^+ on the A-site of BNT,[2] and it is known that better piezoelectric and/or strain properties at the MPB region between BNT rhombohedral and BKT tetragonal phases near $x = 0.16–0.20$ can be achieved.[9–11] The dielectric constant of the BNKT ceramic was reported to be 1030.[10] The good piezoelectric coefficients ($d_{33} = 151$ pC N^{-1}, $d_{31} = 46.9$ pC N^{-1}) were obtained at the optimal composition of $x = 0.20$.[10,12]

It is known that the energy harvesting performances of piezoelectric materials are closely related to their piezoelectric coefficient ($d_{33} \propto \varepsilon P_r$).[13] Thus, a higher remanent polarization (P_r) is desirable for achieving better performances of piezoelectric energy harvesting devices.[14] In order to improve the ferroelectric and piezoelectric properties of the BNKT ceramic to achieve excellent energy harvesting devices, it has been modified with other materials, such as ZnO. The ZnO particle has been widely used as a sintering aid in many dielectric and piezoelectric ceramics.[15] As demonstrated in many studies, the addition of ZnO could improve densification for a wide range of dielectric and ferroelectric materials.[15–18] For example, Promsawat *et al.*[15] reported that the ZnO additive helped to facilitate the densification process and thereby improved the electrical properties of the PMNT ceramics. Lee *et al.*[16] found that the addition of ZnO improved the piezoelectric properties of the $Bi_{0.5}Na_{0.5}TiO_3$ (BNT) ceramics. The effect of ZnO addition on the electrical properties of the $(K_{0.44}Na_{0.52}Li_{0.04})(Nb_{0.86}Ta_{0.10}Sb_{0.04})O_3$ or KNL–NTS ceramics was investigated by Marcos *et al.*[17] They also reported that ZnO doping produced an increase in the ferroelectric performance of the KNL–NTS ceramics. Zhang *et al.*[18] also found that the addition of ZnO could enhance both the ferroelectric and piezoelectric properties of the $0.94Bi_{0.5}Na_{0.5}TiO_3$–$0.06BaTiO_3$ or BNT–6BT ceramics. The maximum P_r and low-field d_{33} values were observed for the BNT–6BT:0.04ZnO ceramics.

For piezoelectric applications, the depolarization temperature (T_d) of BNT-based ceramics is an important factor.[18,19] Many authors have suggested that piezoceramics with a high T_d can be used in a wider range of temperatures because they are more stable. Therefore, several authors have focused on variables that relate to or influence T_d.[20,21] Numerous methods, including doping, the formation of solid solutions, the formation of composites, and the modulation of crystallographic orientation in texturing ceramics, have been found to affect the T_d value.[22–28] However, it should be noted that an effort to raise T_d often leads to a drop in the value of the piezoelectric d_{33}. This tendency restricts the use of the materials in many applications. Therefore, the work to improve the T_d and piezoelectric characteristics of materials based on BNT is still challenging and worthy of continuing research.

It has been proposed that annealing gives several advantages for ferroelectric and piezoelectric characteristics, including those of lead-based piezoelectric ceramics and, more recently, lead-free piezoelectric ceramics.[29,30] Xu *et al.*[31] reported that annealing treatment improved the piezoelectric properties of the $0.95(Bi_{0.5}Na_{0.5})_{0.97}(Li_{0.5}Nd_{0.5})_{0.03}TiO_3$–$0.05BaTiO_3$ or BNTLN0.03–BT5 ceramics. It also induced subtle structural changes. The microstructures of annealed samples become homogeneous, which leads to the disappearance of the Maxwell–Wagner relaxor. The optimal piezoelectric properties of $d_{33} = 148$ pC N^{-1} and $k_p = 0.33$ have been obtained by annealing at 900 °C. Wang *et al.*[32] also reported that good ferroelectric and piezoelectric properties were obtained in the $Na_{0.5}K_{0.5}NbO_3$ ceramics after annealing at 900 °C for 4 h dwell time in an air atmosphere. Since annealing has several benefits for the ferroelectric characteristics, it is anticipated that this technique should have a positive effect on the T_d and other properties such as piezoelectric and energy harvesting properties. In the present investigation, the annealing process was then utilized for the modified BNKT ceramics (BNKT added with ZnO). The effect of thermal annealing on phase evolution, microstructural, dielectric, T_d, ferroelectric, piezoelectric, and energy harvesting properties was investigated and discussed in detail.

2 Experimental

The lead-free ceramic with the composition $Bi_{0.5}(Na_{0.84}K_{0.16})_{0.5}TiO_3$ or BNKT was synthesized by a solid-state reaction method. The starting materials used in this study were the reagent-grade powders of Bi_2O_3, Na_2CO_3, K_2CO_3, TiO_2, and ZnO nanoparticles. All carbonate powders were first dried at 120 °C for 24 h to remove any moisture. The carbonate and high-purity oxide starting materials were weighed based on a stoichiometric formula of $Bi_{0.5}(Na_{0.84}K_{0.16})_{0.5}TiO_3$ and then mixed and ball milled in a 99.9% ethanol solution for 24 h. The slurries were dried in an oven for 24 h at a temperature of 120 °C. Dried BNKT powder was calcined in a closed alumina crucible at 900 °C for 2 h with a heating/cooling rate of 5 °C min^{-1}. After calcination, the ZnO nanoparticles (less than 100 nm) were added into the calcined BNKT powder and then milled again in ethanol for 24 h with the formula of $Bi_{0.5}(Na_{0.84}K_{0.16})_{0.5}TiO_3$/0.01ZnO referred to as the BNKT/0.01ZnO. After drying and sieving, the mixed powders were granulated by adding a few drops of 4 wt% PVA as a binder and then pressed into disks with a diameter of 10 mm and a thickness of about 1.3 mm. The pellets were then preheated in the air at 500 °C for 1 h to remove the organic binder and then sintered at 1125 °C for 2 h dwell time with a heating/cooling rate of 5 °C min^{-1} in closed alumina crucibles. To minimize the loss of the volatile elements, the green pellets were embedded in a powder of the same composition. In order to further improve the quality of the ceramics, the sintered ceramics were annealed at 950 °C with a heating/cooling rate of 5 °C min^{-1} and various annealing times of 0, 4, 8, and 12 h in an air atmosphere, respectively.

The bulk density of all ceramics was determined using Archimedes' method. An X-ray diffractometer (XRD, PANalytical, X′ Pert ProMPD) was used to identify the phase of all sintered ceramics. The Raman spectra were carried out on the polished sintered pellets and recorded by Raman spectroscopy (T6400 JY, Horiba Jobin Yvon). The surface morphologies of the sintered ceramics were observed using a field-emission scanning electron microscope (FE-SEM, JEOL JSM-6335F). The average grain size of each sample was determined by a mean linear interception method from the SEM micrographs. For

electrical measurements, all samples were polished to 1 mm thickness, and high-temperature silver paste was fired on both sides at 700 °C for 30 min in order to form the electrodes. Temperature dependence of dielectric properties was also carried out using a 4192A LCR-meter connected to a high-temperature furnace from room temperature (RT) to 500 °C with various frequency ranges of 1–1000 kHz. A radiant precision ferroelectric tester was used to investigate the ferroelectric properties at both room temperature (RT) and high temperatures (HT) of 25–150 °C. Various AC electric fields of 30–65 kV cm^{-1} at a frequency of 0.1 Hz were utilized in the hysteresis measurement. For piezoelectric characterization, the samples were poled in silicone oil under a DC electric field of 5 kV mm^{-1} for 15 min at RT. The piezoelectric coefficient (d_{33}) was measured after aging the ceramics for at least 24 h using a d_{33} meter (KCF technologies, S5865) at a frequency of 50 Hz. The planar electromechanical coupling factor (k_p) was measured by the resonance and anti-resonance technique using an impedance analyzer (HP 4284A). The piezoelectric voltage constant (g_{33}) and the off-resonance figure of merit (FoM) for energy harvesting were also calculated in this study.

3 Results and discussion

3.1 Densification and phase evolution

In this experiment, the density as a function of annealing times (0–12 h) of the BNKT/0.01ZnO ceramics was determined, and the values are listed in Table 1. The density increased from 5.81 g cm^{-3} for the unannealed ceramic to the maximum value of 5.86 g cm^{-3} for the 8 h annealed ceramic, and then slightly decreased to 5.84 g cm^{-3} for the 12 h annealed ceramic. The annealing process and ZnO additives can help to improve the densification of all ceramics. However, the slightly lower density value after 12 h of annealing may be caused by the high volatilization of some components for overtime annealing,[32] such as Bi and K. The high-density sample was responsible for the improved electrical characteristics,[29,33] as shown by the results in the next section.

In order to check the phase-purity and structural parameters, all ceramics were investigated by the X-ray diffraction technique at RT,[33] and the XRD pattern of the BNKT/0.01ZnO ceramics annealed at 950 °C with different annealing times, where 2θ = 20–70° is shown in Fig. 1(a). It is noted that all annealed ceramics exhibited a single perovskite structure without any detectable impurity peaks, indicating that ZnO had diffused into the BNKT lattice to form a complete solid solution. The results of a more detailed XRD analysis performed in a narrow range of 2θ = 39–41° and 2θ = 44–48° are shown in Fig. 1(b) and (c), respectively. Based on peak profile fitting, the unannealed ceramic exhibited the morphotropic phase boundary (MPB) structure, consisting of rhombohedral and tetragonal phases.

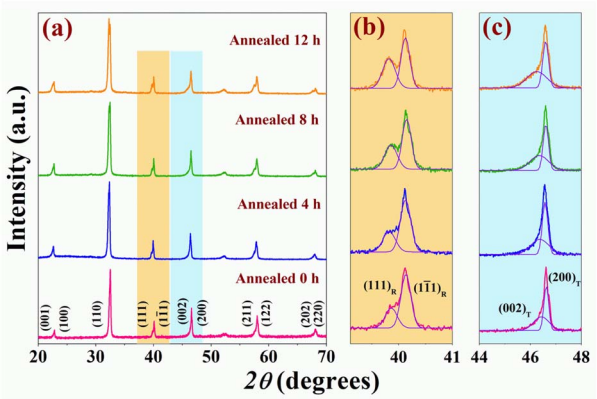

Fig. 1 X-ray diffraction patterns of the BNKT/0.01ZnO ceramics annealed at 950 °C with different annealing times, where (a) 2θ = 20–70° (b) 2θ = 39–41°, and (c) 2θ = 44–48°.

This was evidenced by a slight splitting of $(111)_R/(1\bar{1}1)_R$ rhombohedral peaks at $2\theta \sim 40°$ and $(002)_T/(200)_T$ tetragonal peaks at $2\theta \sim 46.5°$. This result is also consistent with the work done by Sasaki *et al.*[10] on the $(1-y)$BNT–yBKT ceramics, who found a relatively broad MPB region in the range of y = 0.16–0.20 between BNT rhombohedral and BKT tetragonal ceramics. This result also agrees with the previous experiments.[12,34,35] However, the weak splitting of the (200) peak indicates the rhombohedral rich phase. It should be noted that with a further increase in the annealing time up to 8–12 h, XRD displayed more splitting of $(111)_R/(1\bar{1}1)_R$ rhombohedral peaks and $(002)_T/(200)_T$ tetragonal peaks. The phase transition from the mixed rhombohedral–tetragonal to a more tetragonal phase portion was observed when the annealing time was increased. To check this, the $c/a - 1$ value (where c/a is tetragonally) was calculated (Table 1). The $c/a - 1$ value increased as the annealing time increased, confirming the increase in the tetragonal phase.

The full width at half maximum (FWHM) values using a certain XRD peak for all ceramics were determined in this investigation.[36,37] In the present work, the FWHM value was calculated from the (110) reflection main peak in the X-ray diffraction pattern, and the values are also included in Table 1. The FWHM of the (110) peaks of the annealed ceramics (4–12 h) was much smaller than that of the unannealed ceramics (0 h), suggesting that annealing improved the degree of

Table 1 Physical, microstructure and mechanical properties of the BNKT/0.01ZnO ceramics annealed at 950 °C with different annealing times

Annealing time (h)	Density (g cm^{-3})	Phase	c/a	$c/a - 1$	FWHM of (110) (°)	Crystallite size (nm)	Average grain size (μm)
0	5.81	R + T	1.0037	0.0037	0.66	12.54	1.44 ± 0.21
4	5.82	R + T	1.0049	0.0049	0.60	13.80	1.59 ± 0.25
8	5.86	R + T	1.0066	0.0066	0.57	14.52	1.98 ± 0.23
12	5.84	R + T	1.0090	0.0090	0.55	15.05	2.28 ± 0.19

crystallinity of the samples. The crystallite size (D) was also used to check the degree of crystallinity of the ceramics. In the current work, the X-ray peak broadening (110) reflection was selected for this proposed, and the calculation was performed based on the Debye–Scherrer formula:[37]

$$D = \frac{k\lambda}{B\cos\theta} \quad (1)$$

where λ is taken to be 0.15418 nm as the X-ray source is Cu-Kα, B is the full width at half maximum (FWHM), k is a fixed number 0.9, and θ is the Bragg's angle.[38–43] It can be seen that crystallite size increased from 12.54 nm for the unannealed ceramic to the maximum value of 15.05 nm for the 12 h annealed ceramic. With increasing annealing time, the FWHM of the (110) peak became narrower and the crystallite size increased, indicating an improvement in the degree of crystallinity of the annealed ceramics.[40] Furthermore, the lower FWHM value (with increasing annealing time) also indicated a better homogeneous chemical distribution in the ceramics.[44,45] In addition, it was proposed that the increase in crystallite size could be accompanied by an improvement in the ceramic's electrical properties.[41,43]

To further analyze the evolution of the crystal structure with varying annealing times, Raman spectra were measured in the range of 100–1200 cm^{-1}, which are now presented in Fig. 2. Obviously, four main regions could be detected in the spectrum at room temperature (RT), which is nearly identical to those previously reported data of BNT-based ceramics:[46–50] (1) the mode located below 200 cm^{-1} associated with the vibration of perovskite A-site, (2) the around 300 cm^{-1} modes should be related to Ti–O vibrations, (3) the modes approximately 450–650 cm^{-1} related to TiO_6-octahedra vibration, and (4) the modes over 700 cm^{-1} related to the A_1 (longitudinal optical) and E (longitudinal optical) overlapping bands.[47] The Raman peaks at the mode located below 200 cm^{-1} slightly shifted towards the lower wavenumber for the 8–12 h ceramics. This may be linked with the volatilization of A-site ions for a longer annealing time. The broader and splitting peak of the mode around 300 cm^{-1} and 450–650 cm^{-1} was observed with increasing annealing time which corresponds to a higher degree of tetragonally. This result agrees well with previous studies.[46,48] Overall, spectra recorded for the studied ceramics are in good agreement with that of the previously reported for other BNT-based ceramics which had a coexisted phase structure between rhombohedral ($R3c$) and tetragonal ($P4bm$) phases.[51] This Raman result also agrees well with the XRD analysis.

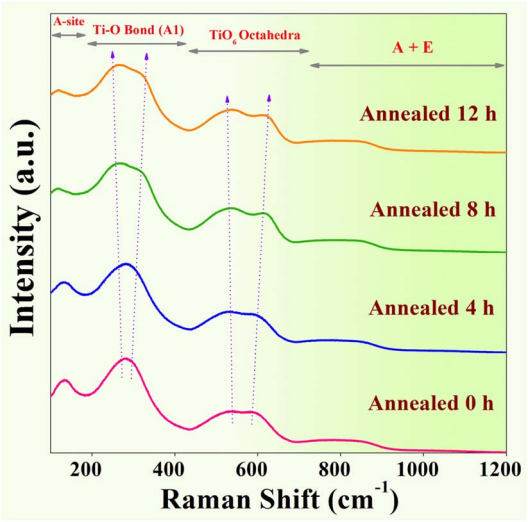

Fig. 2 Raman spectra at room temperature of the BNKT/0.01ZnO ceramics annealed at 950 °C with different annealing times.

3.2 Microstructure analysis

Microstructural development during the annealing process was investigated by scanning electron microscopy (SEM). The FE-SEM micrographs of sintered surfaces of the BNKT/0.01ZnO ceramics annealed at 950 °C with different annealing times are shown in Fig. 3. The average grain size of each sample is given in Table 1. It is evident that all ceramics were very dense, smooth, and crack free. The grain was well-crystallized with clear grain boundaries and contained a cubic-like shape. The SEM micrographs clearly showed that the annealing time had an influence on the microstructure of the BNKT/0.01ZnO ceramics. The average grain size increased with increasing annealing time. The average grain size of the unannealed ceramic was found to be 1.44 ± 0.21 μm. The average grain size initially increased with the annealing time and reached a maximum value of 2.28 ± 0.19 μm for the 12 h annealed ceramic. Similar behavior was also reported in a recent investigation.[52] As the annealing time increased, the grains grew and the average grain size increased, whereas the number and size of the pores decreased. In the current study, a line intercept method was used to find out the average grain size. It should be noted that the percentage increase in grain size for this study is 44% after 12 h of annealing. Fig. 4(a) displays plots of FWHM *versus* crystallite size and grain size. It was found that the crystallite size had a linearly decreasing trend with FWHM, while grain size had an exponential decay with FWHM. A relation between crystallite size and grain size is also presented in

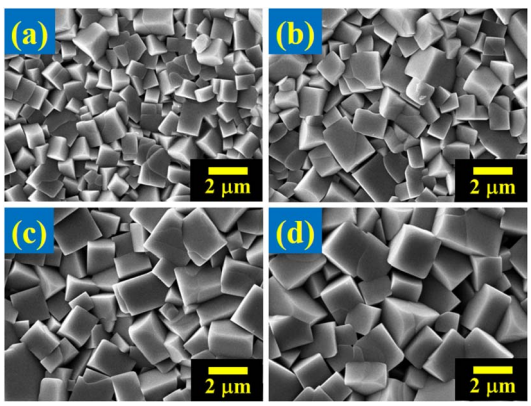

Fig. 3 The FE-SEM micrographs with as sintered surfaces of the BNKT/0.01ZnO ceramics annealed at 950 °C with different annealing times, where (a) 0 h, (b) 4 h, (c) 8 h, and (d) 12 h.

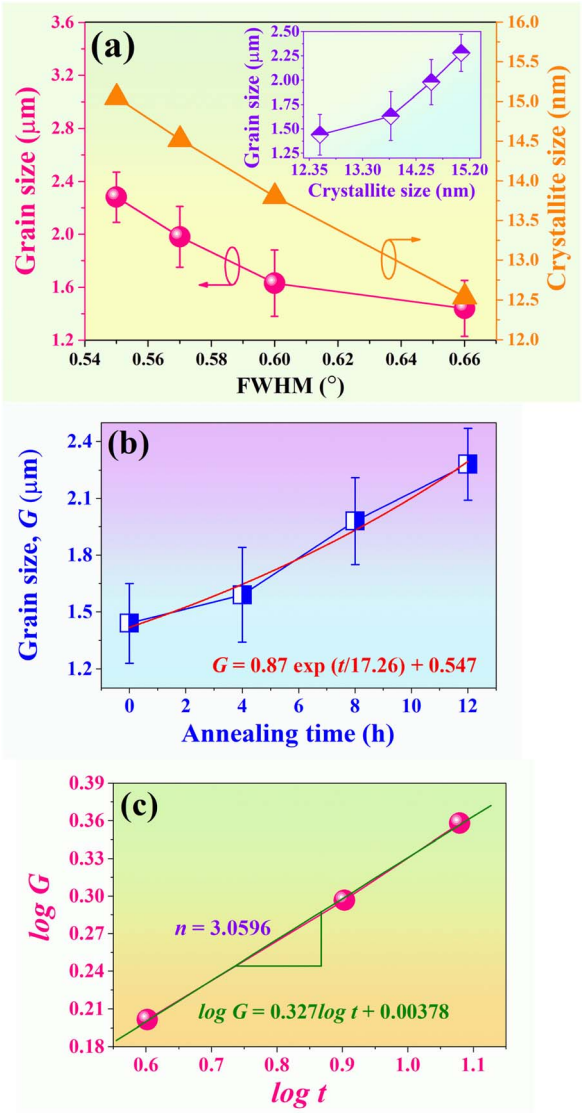

Fig. 4 Plots of (a) FWHM *versus* grain size and crystallite size (inset shows a relation between grain size and crystallite size), (b) grain size as a function of annealing time, and (c) log G as a function of log t.

the inset of Fig. 4(a). As crystallite size increased, grain size increased exponentially. Therefore, the obtained data indicated that annealing enhanced both crystallite size and grain size. In the present experiment, the grain size increased exponentially with increasing annealing time, as seen in Fig. 4(b). Normal grain growth can be explained by the phenomenological kinetic grain growth equation, which is written as:[4]

$$\log G = \frac{1}{n}\log t + \frac{1}{n}\left[\log K_0 - 0.434\frac{Q}{RT}\right] \quad (2)$$

where G is the average grain size at the time t, n is the kinetic grain growth exponent, K_0 is the constant, Q is the apparent activation energy, R is the gas constant, and T is the absolute temperature. It was noted from the equation that the average grain size was an exponential function of the annealing time (t) (Fig. 4(b)). To compare the experimental result with the kinetic equation better, log G is plotted *versus* log t, and there generally exists a reasonably good linear relationship between log G and log t (Fig. 4(c)), which is consistent with eqn (2).[4] Based on Fig. 4(b), a reasonably good linear relationship between log G and log t was observed, where the slope is $1/n$. Generally, a small n value indicates a large grain growth rate, which can be shown by differentiating eqn (2). The n value for this study was found to be 3.05. Therefore, the small n value calculation indicated that the annealing produced a moderate grain growth rate[53,54] with increasing annealing time. The relationships between the grain size and the electrical properties (*i.e.*, dielectric, ferroelectric, and piezoelectric) will be discussed in the next sections. As is known, grain size has a significant influence on the dielectric characteristics and polarization of piezoelectric materials.[9,55]

3.3 Dielectric properties

The room temperature dielectric constant (ε_r) and dielectric loss (tan δ) at a frequency of 1 kHz are listed in Table 2. The ε_r of the un-annealed ceramic was found to be 501 with tan δ of 0.0425. The ε_r initially increased with the annealing time and reached a maximum value of 651 for the 8 h annealed ceramic, and then slightly decreased to 529 for the 12 h annealed ceramic. The density is believed to be an important factor in the higher electrical properties of the samples,[33] *i.e.*, higher density resulted in higher dielectric properties.

Temperature dependence on the dielectric constant (ε_r) and dielectric loss (tan δ) of the poled BNKT/0.01ZnO ceramics annealed at 950 °C with different annealing times, and measurements at various frequencies from 1–1000 kHz are shown in Fig. 5. The related dielectric properties are also summarized in Table 2. There were two dielectric anomalous peaks in the ε_r–T plot. The first dielectric anomaly peak (shoulder peak), characterized by a large dielectric peak and noticeable frequency dispersion, was noted at a temperature below 200 °C. This temperature corresponds to T_s, indicating the relaxor ferroelectrics which are usually caused by the thermal evolutions of discrete polar nanoregions.[6] The secondary anomaly broadened peak, at T_m, indicates the maximum dielectric constant (ε_m) in ε_r *vs.* T plots. The two dielectric anomalous peaks on the dielectric permittivity curves have been commonly reported in BNT-based systems.[56–58] Based on Fig. 6(a), the unannealed ceramic had the ε_{max} of 4836. The ε_{max} increased with the annealing time and reached a maximum value of 5551 for the 8 h annealed ceramic. At temperature ≥150 °C, there was a dispersion in tan δ value with frequency. However, the degree of dispersion was lower than that reported in other lead-free materials such as the $(Bi_{0.5}Na_{0.5})TiO_3$–$BaTiO_3$ system.[33] From Fig. 5, the tan δ value at T_m for all ceramics was in the range 0.03–0.04, which is acceptable for a characteristic of capacitors at a high temperature.

The reasons for the observed increase in the dielectric characteristics (by annealing) are complex due to the possibility of it being affected by many factors. Xia and Yao[59] suggested that the observed increases in dielectric characteristics for

Table 2 Dielectric properties obtained at HT (25–500 °C) and a frequency of 1 kHz of the BNKT/0.01ZnO ceramics annealed at 950 °C with different annealing times

Annealing time (h)	ε_r	tan δ^a	T_{F-R} (°C)	T_m (°C)	ε_{max}	tan δ^b	T_B (°C)	$\Delta T = T_B - T_m$ (°C)	γ	T_d (°C)
0	501	0.0425	168.25	307.18	4836	0.0334	369.44	62.26	1.48	157.22
4	536	0.0471	167.60	306.20	5437	0.0363	368.33	62.13	1.46	156.17
8	651	0.0503	167.38	305.41	5551	0.0387	367.15	61.74	1.43	155.98
12	529	0.0443	166.41	305.24	5501	0.0384	366.65	61.41	1.39	155.89

[a] Dielectric loss (tan δ) measured at T = RT and a frequency of 1 kHz. [b] Dielectric loss (tan δ) measured at $T = T_m$ and a frequency of 1 kHz.

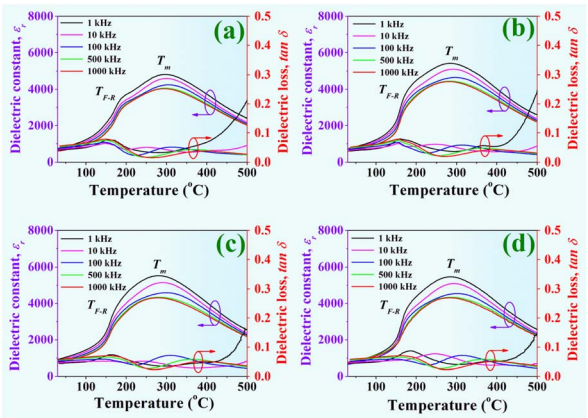

Fig. 5 Temperature dependence on dielectric constant (ε_r) and dielectric loss (tan δ) of the poled BNKT/0.01ZnO ceramics annealed at 950 °C with different annealing times, measurement at various frequencies from 1–1000 kHz, where (a) 0 h, (b) 4 h, (c) 8 h, and (d) 12 h.

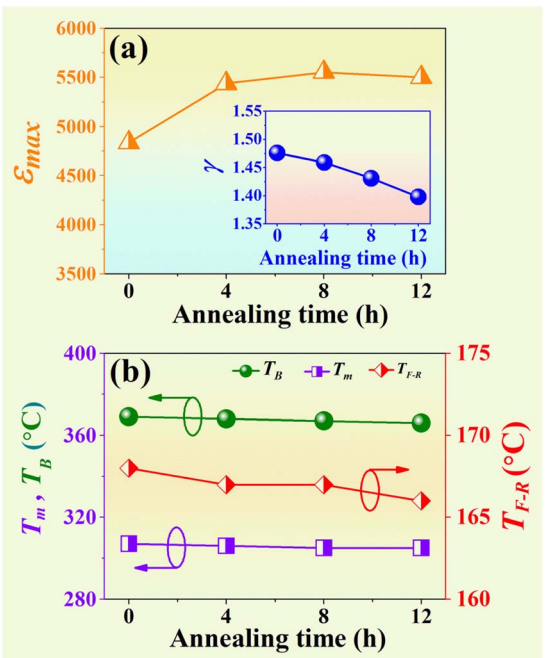

Fig. 6 Plot of (a) ε_{max} as a function of annealing time (inset: the γ value as various annealing times), and (b) T_m, T_B, and T_{F-R} values as a function of annealing time.

$Pb(Zn_{1/3}Nb_{2/3})O_3$ (by annealing) are mostly attributable to many factors: (1) grain size change, (2) density change, (3) internal stress release, (4) a change in the content of the secondary phase, (5) the grain boundary layer, (6) the defect, (7) domain wall motion, and (8) a change in the order degree of B-site ions.[59] However, it should be noted that the effect of grain size can be linked to a variety of factors, such as domain wall motion, internal stress release, and grain boundary layer characteristics. For the grain size effect, Mudinepalli *et al.*[60] investigated the properties of BT based ceramics ($Ba_{0.8}Sr_{0.2}TiO_3$) and proposed that the dielectric constant is affected by domain population and domain wall mobility. They also proposed that a uniform grain size (big grains) can reduce internal stress, making it easy and regular for the domain walls to move, which raises the dielectric constant.[60] Zhao *et al.*[61] reported that the critical grain size for the disappearance of ferroelectricity in BT ceramics is 10–30 nm. Furthermore, the strong broadening in the permittivity curve of their fine grain ceramics was explained by the size effect and the effect of a low-permittivity non-ferroelectric layer at the grain boundary. These effects depend on the grain size.[15,61]

It is known that piezoceramics with their composition near the MPB composition often present high electrical properties such as high dielectric and piezoelectric properties. This is due to the formation of a mixture phase such as that of the rhombohedral and tetragonal phases which have a larger number of reorientable polarization directions. Therefore, the improvement in the dielectric constant of the 8 h annealed ceramic in the present study may be attributed to the formation of the mixture phase between rhombohedral and tetragonal with an optimal fraction that has better optimal properties. Furthermore, the increase in grain size, degree of composition homogeneity, and density also contributed to the improvement. In addition, it should be noted that the studied was added with BT, and BT ceramics need a high sintering temperature (as compared to BNT ceramics) to achieve the best combination of density and properties. Thus, annealing can help optimize the properties of the ceramics. However, the change in the amount of the secondary phase has less effect since the studied ceramics presented no secondary phase. For the ceramics annealed at 12 h, the ε_{max} slightly decreased to 5501. This result may be linked to the volatilization of some components for a longer annealing time (*i.e.*, Bi and K).[30,32] This can be linked with

a slight decrease in density and a slight decrease in the dielectric constant of this ceramic.

3.4 Phase transition behavior

For phase transition temperatures, the T_m value was corrected from the dielectric data as presented in the previous section. The T_m value slightly shifted down by ~2 °C with increasing annealing time up to 12 h (Fig. 6(b) and Table 2). The Burn's temperature (T_B) value was also evaluated for the current investigation. Normally, at high temperatures, relaxors exist in a nonpolar paraelectric phase analogous to the ferroelectric paraelectric phase. However, as the temperature drops below the Burns temperature (T_B), they undergo a transformation into an ergodic relaxor (ER) state. This temperature indicates the start of the polarization process in relaxors.[62] To determine the T_B, there are many techniques, such as the refractive index,[62,63] electrostrictive strain,[64] or deviation from the Curie–Weiss behavior.[62] In the present investigation, the T_B was collected from the dielectric constant that starts to deviate from the Curie–Weiss law.[65] The plot of the inverse dielectric permittivity ($1/\varepsilon_r$) as a function of temperature at 1 kHz that was used to determine the T_B values is shown in the supplementary information in Fig. S1.† Based on Fig. 6(b) and Table 2, the T_B also slightly decreased from 369 °C for the unannealed ceramic to 366 °C for the 12 h annealed ceramic (*i.e.* a decrease by 3 °C). In addition, the deviation from the Curie–Weiss law can be depicted by ΔT (degree of deviation) as follows: $\Delta T = T_B - T_m$.[66] The calculated values of ΔT as a function of annealing time are also listed in Table 2. The ΔT values were 62 to 61 °C, which indicated that the degree of diffuse phase transition is moderate. For 12 h annealing, the ΔT decreased by 1 °C, implying that the annealing time had less effect on the degree of deviation for the studied ceramics.[67]

To further confirm the diffuseness of phase transition, the modified Curie–Weiss law is used, which is given in the following equation:[6,62,65,68,69]

$$\frac{1}{\varepsilon_r} - \frac{1}{\varepsilon_m} = \frac{(T - T_m)^\gamma}{C'} \quad (3)$$

where γ is the degree of diffuseness, C' is Curie-like constant, T_m is the temperature of the maximum dielectric constant, ε_r is the dielectric constant, and ε_m is the maximum dielectric constant at T_m. The value of γ can be calculated from the slope of the fitting curves.[6] A higher γ value indicates a stronger degree of diffuse phase transition. The slope of the fitting curve of $\ln(1/\varepsilon_r - 1/\varepsilon_m)$ *vs.* $\ln(T - T_m)$ according to eqn (3) is used to determine the γ value. A linear relationship is observed for all compositions.[70] According to the γ value in Table 2 and the inset of Fig. 6(a), the γ value shows a slight change from 1.48 for the unannealed ceramic to 1.39 for the 12 h annealed ceramic. Thus, the annealing did not affect the diffuse phase transition too much.

3.5 Depolarization temperature (T_d)

To determine the T_d value, many techniques have been proposed.[71] In the current study, the thermally stimulated depolarization current (TSDC) technique was employed. Plots of the current density–temperature (J–T) from the TSDC technique of the BNKT/0.01ZnO ceramics annealed at 950 °C with different annealing times are shown in Fig. 7. The T_d value is also summarized in Table 2. It was found that the annealing time had no significant effect on the change of the T_d value since the T_d was slightly shifted down from 157 °C for the unannealed ceramic to 156 °C for the 12 h annealed ceramic. To confirm the trend of the value, the T_{F-R} value was determined at a discontinuous change in dielectric loss (a small sharp peak at temperature ≤150 °C) in dielectric temperature spectra of the poled ceramics (Table 2). This temperature implies ferroelectric-relaxor transition upon heating.[56] The T_{F-R} value decreased from 168 to 166 °C after annealing for 12 h (*i.e.* a decrease of 2 °C). To double check the TSDC result, another different technique was performed. For this purpose, a measurement of the electromechanical coupling coefficient (k_p) was carried out at a range of temperatures.[72,73] The resulting shifting T_d value is shown in the ESI (Fig. S2†). It was found that the T_d value slightly decreased by 2 °C after annealing for 12 h. This result is consistent with the TDSC result.

To explain the shift in T_d value, numerous hypotheses and models have been proposed, such as the ion doping model, the charge compensation model, and the stress field model. For the ion doping model, several authors have proposed that some dopant ions can diffuse into the host lattice during processing, hence promoting a more stable ferroelectric phase and causing the T_d value to increase.[19,74–77] Mahajan *et al.*[75] also proposed that thermal depolarization behavior is considered to be strongly connected to the rhombohedral–tetragonal phase temperature. Li *et al.*[76] found that the direct doping of Zn^{2+} into 0.94BNT–0.06BT may delay the thermal depolarization produced by the reformation of a long-range ferroelectric order due to the high polarizability of the Zn ion. This would cause a large dipole moment of the BO_6 octahedra, enhance the coherence of neighboring dipoles, and inhibit the ferroelectric-relaxor transition. However, the diffusion of dopant ions can have a negative effect, *i.e.*, it can cause composition and charge

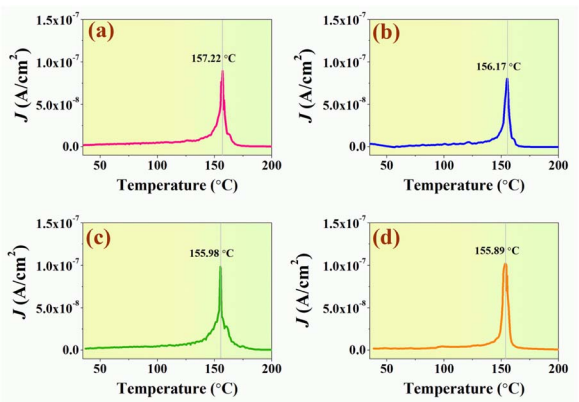

Fig. 7 Plots current density–temperature (J–T) from the TSDC technique of the BNKT/0.01ZnO ceramics annealed at 950 °C with different annealing times, where (a) 0 h, (b) 4 h, (c) 8 h, and (d) 12 h.

disorder, hence destabilizing the ferroelectric ordering in the samples. Some composites consisting of piezoelectric and semiconductor phases, such as the $0.94Bi_{0.5}Na_{0.5}TiO_3$–$0.06BaTiO_3$/$x$ZnO (BNT–6BT/$x$ZnO) composites, for which ZnO is the semiconductor phase, were suggested using such a charge compensation model.[18] In this case, the application of an external electric field causes a redistribution of the charges in the semiconductor ZnO at the interface between ZnO and BNT–BT. This provides a local electric field to compensate for the ferroelectric depolarization field when the external field is removed, hence stabilizing ferroelectric domains in composites.[18]

The stress field model was proposed for many studies on BNT-based ceramics, adding ZnO.[75,78] For this model, it is believed that the thermal deviatoric stresses in a composite are caused by the difference in the coefficients of thermal expansion between ZnO and BNT–BT. This helps to stabilize the ferroelectric phase and broaden the temperature range of depolarization. This model has also been used to explain the increasing trend of T_d in many composites such as $Bi_{0.5}(Na_{0.8}K_{0.2})_{0.5}TiO_3$:$Al_2O_3$ (BNKT:Al_2O_3).[27] The creation of oxygen vacancies, as reported in many experiments, can raise the T_d value, due to the domain walls in the grains of the ceramics being clamped. However, this is generally accompanied by a decline in piezoelectric properties.[19] Doping B_2O_3 (as an interstitial dopant) into BNT–BT ceramics can increase the T_d value. This was proposed to be due to the ability of stress generated from doping to stabilize the ferroelectric phase, thus, improving the T_d value.[19] Thomas[79] proposed that the stability of a ferroelectric domain may be reduced if the coupling reaction between the A-site cation and the BO_6 octahedron is weak. This model was utilized to explain the reduction in T_d in a number of publications, which were connected with the weak coupling reaction that took place between the A-site cation and the BO_6 octahedron.[80,81] Furthermore, Nagata *et al.*[82] proposed that the change in rhombohedral distortion affects the rise in T_d in the $0.92BNT–0.08(Bi_{0.5}Li_{0.5})TiO_3$ sample that had been quenched, which was caused by Bi ions being off-center. Khatua *et al.*[83] reported an increase in T_d value without a significant loss of piezoelectricity by grain size effect. They suggested the ferroelectric distortion of the field stabilized ferroelectric phase is dependent on the grain size.

In the current study, the reason for the improvements in piezoelectric properties (see next section) with the slight change in T_d is complex. It could be for a variety of reasons. Normally, the annealing process would result in the formation of oxygen vacancies, which often leads to an increase in T_d value, but will also be followed by a reduction in piezoelectric properties. However, for the present investigation, it is believed that the formation of oxygen vacancies is not too great because the annealing temperature is not too high. Therefore, the T_d value slightly changed. Furthermore, ZnO was added to the studied ceramics. For the ZnO additive, it has been proposed that Zn ions can enter the lattices of many ceramic systems and then help stabilize the ferroelectric ordering.[76] In addition, annealing improved ferroelectric properties by obtaining the optimal portion of the mixture phase and increasing grain size (see the following sections).

3.6 Ferroelectric properties

Normally, there are many factors affecting the characteristics of the ferroelectric hysteresis loop, which are associated with the material itself and the measurement conditions.[84] In the current experiment, the polarization–electric field (P–E) hysteresis loop of the BNKT/0.01ZnO ceramics was measured at RT with different annealing times of 0–12 h, and under various electric fields of 30–65 kV cm^{-1}, as shown in Fig. 8. The related ferroelectric properties are summarized in Table 3. It was found that the maximum polarization (P_{max}), remanent polarization (P_r), and coercive field (E_c) values increased with an increase the applied electric field for all ceramics (Fig. 9(a) and (b)). At 30 kV cm^{-1} (Fig. 8), all ceramics showed an ellipse-like shape loop. This indicates a near-linear relationship of P–E, where it is known that some low electric fields are not enough to switch the domains.[85] However, the polarization nonlinearity was developed in both the positive and negative field zones at 40 kV cm^{-1} electric fields. These results make it clearly evident that the electric field strength of 40 kV cm^{-1} has sufficient energy to constrain the realignment of some domains in the direction of the applied fields. At 65 kV cm^{-1} electric fields, polarization nonlinearity developed in both regions of the positive and negative fields with a well-saturated hysteresis loop. This indicates that the electric fields strength of 65 kV cm^{-1} has enough energy to constrain the realignment of all domains in the direction of the electric field.[85] For an applied field greater than 65 kV cm^{-1}, however, it caused the ceramics to undergo a dielectric breakdown.

At an electric field of 65 kV cm^{-1}, the unannealed ceramic displayed a well-saturated typical P–E hysteresis loop[86] with the P_{max} of 38.06 μC cm^{-2}, P_r of 33.02 μC cm^{-2}, and the E_c of 42.98 kV cm^{-1}, indicating a strong ferroelectric ordering. However,

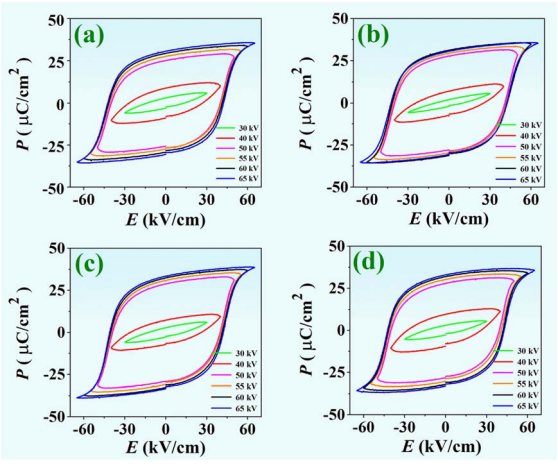

Fig. 8 Polarization–electric field (P–E) hysteresis loop of the BNKT/0.01ZnO ceramics annealed at 950 °C with different annealing times, measured at RT under various electric field of 30–65 kV cm^{-1}, where (a) 0 h, (b) 4 h, (c) 8 h, and (d) 12 h.

Table 3 Ferroelectric, piezoelectric, and energy harvesting properties of the BNKT/0.01ZnO ceramics annealed at 950 °C with different annealing times

Annealing time (h)	P_{max} (μC cm^{-2})	P_r (μC cm^{-2})	E_c (kV cm^{-1})	R_{sq}	d_{33} (pC N^{-1})	k_p	g_{33} (10^{-3} Vm N^{-1})	FoM (pm^2 N^{-1})
0	38.06	33.02	42.98	1.39	151	0.583	34.04	5.14
4	38.31	33.27	42.85	1.40	162	0.586	34.14	5.53
8	41.28	35.85	42.60	1.42	198	0.598	34.35	6.80
12	39.20	35.05	42.58	1.40	165	0.588	35.01	5.74

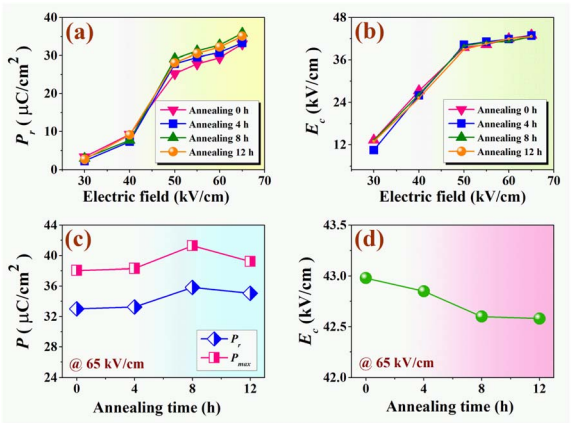

Fig. 9 Plots of (a) P_r, (b) E_c values as a function of electric fields from 30–65 kV cm^{-1}, (c) P_r and P_{max} as a function of annealing time @ E = 65 kV cm^{-1}, and (d) E_c as a function of annealing time @ E = 65 kV cm^{-1} of the BNKT/0.01ZnO ceramics annealed at 950 °C with different annealing times.

the annealing had a significant influence on the P_{max}, P_r and E_c values, *i.e.*, it improved ferroelectric behavior, as seen from an enhancement trend in both the P_r and P_{max} values. The P_r increased from 33.02 μC cm^{-2} for the un-annealed ceramic to 35.85 μC cm^{-2} for the 8 h annealed ceramic and then slightly decreased to 35.05 μC cm^{-2} when the annealing time increased up to 12 h (Fig. 9(c)). In addition, the E_c dropped with an increase in the annealing time (Fig. 9(d)). Normally, the improvement of ferroelectric properties can be related to many factors, as described in the previous section, such as MPB, grain size effect, heterogeneous chemical composition, and density. For this work, it was found that these factors were important factors, and it should be noted that ceramics with higher density and grain size values often have a higher P_r value.[87] The 12 h annealed ceramic, on the other hand, has a lower density and thus a slightly lower P_r value.

For the grain size effect, Hao *et al.*[88] studied the properties of $(Ba_{0.85}Ca_{0.15})(Zr_{0.1}Ti_{0.9})O_3$ and proposed that the fraction of grains responsible for the opposite polarization reverse in ferroelectrics can be expressed using a formula:[88]

$$f = f_0[1 - \exp(-G_a d^3/kT)] \quad (4)$$

where G_a is a constant representing the grain anisotropic energy density, and d is the grain size. This equation illustrates that f is relevant in relation to grain size. Therefore, as grain size increases, the number of grains that contribute to polarization reversals also increases. This increases the ferroelectricity of the ceramics.[88] For $BaTiO_3$, Zhao *et al.*[61] reported a relationship between grain size and the tetragonal distortion (η), where $\eta = c/a - 1$. They also proposed that P_s can have a relation with η as the following equation shows:[61]

$$P_s^2 = \frac{\eta}{k} \quad (5)$$

and k is a coefficient that relates to the electrostrictive coefficients, and P_s is saturated polarization. When grain size increases, the P_s^2 thus also increases. In the current work, however, the increase in η or $c/a - 1$ value indicates the increase in tetragonally of mixture phase (between rhombohedral and tetragonal). Therefore, annealing produced a good fraction of these phases and gave better or optimal ferroelectric properties.

To check the degree of improvement of the ferroelectric performance, the loop squareness (R_{sq}) may be an indicator for this. Haertling *et al.*[89] used the squareness to measure not only the deviation in the polarization axis but also that in the electric field axis with the following empirical equation:[90–92]

$$R_{sq} = \frac{P_r}{P_s} + \frac{P_{1.1E_c}}{P_r} \quad (6)$$

where P_r is remanent polarization, P_s is saturated polarization and E_c is coercive field. The $P_{1.1E_c}$ is the polarization at an electric field equal to 1.1 times of E_c.[91] This equation can be used to quantify the changes in hysteresis behavior. For an ideal hysteresis loop, R_{sq} is equal to 2.0. Based on the on the obtained data (Table 3), the R_{sq} increased with increasing annealing time, thereby confirming the improvement of ferroelectric performance. Therefore, the ferroelectric properties of the BNKT/0.01ZnO ceramics could be enhanced by optimizing annealing times.

Temperature dependence of polarization–electric field (P–E) hysteresis loops of the BNKT/0.01ZnO ceramics annealed at 950 °C with different annealing times, measured under an electric field of 65 kV cm^{-1} and a frequency of 0.1 kHz are shown in the ESI in Fig. S3.† All ceramics exhibited well-saturated P–E loops at RT (25 °C). With the increasing temperature up to 125 °C, the P_r and E_c values decreased, and the hysteresis loops started to deform and showed constricted loops for all samples at 150 °C. It was confirmed that the high temperature (~150 °C) can cause lattice distortion and disrupt the ferroelectric long-range order, leading to a decrease in the polarization states.[93] The decrease of P_r and E_c values with increasing temperature (Fig. S4(a) and S4(b)†) is consistent with

that reported by Li *et al.*[94] in the $0.94(Bi_{0.5}Na_{0.5})TiO_3$–$0.06BaTiO_3$ (BNTBT6) lead-free ceramics. They reported that the P_r and E_c decreased significantly after 96 °C, and then a pinched hysteresis was obtained with the increasing temperature. The change of ferroelectric (FE) ordering, and a phase transition from ferroelectric (FE) to ergodic relaxor (RE) were thus observed.

3.7 Piezoelectric properties

Plots of the piezoelectric coefficient (d_{33}) value of the BNKT/0.01ZnO ceramics at different annealing times are shown in Fig. 10. The related values are also listed in Table 3. The d_{33} value of the unannealed ceramic in this study was 151 pC N^{-1}. The d_{33} increased with an increase in the annealing time and achieved the maximum value of 198 pC N^{-1} for the 8 h annealed ceramic. However, as the annealing time increased to 12 h, these values decreased slightly. The planar electromechanical coupling coefficient (k_p) for this experiment was determined from measured values guided by the following formula:[4,95,96]

$$k_p = \sqrt{2.51 \times \left(\frac{f_a - f_r}{f_r}\right)} \quad (7)$$

where f_r and f_a are the resonance and anti-resonance frequencies, respectively.[95] In this work, the maximum k_p of 0.598 was also obtained for the 8 h annealed ceramic (see Table 3). Normally, the improvements of d_{33} and k_p for many piezoelectric ceramics can be related to many factors. The grain size effect is one of them. Kang *et al.*[97] argued that the poling efficiency rose with increasing grain size in the case of lead-free ceramics, such as in the $Pb_{0.9}La_{0.1}TiO_3$ system, which was attributable to improving the facility of 90° domain switching. They also proposed that, as the increase in grain size, it would be expected to enhance the domain switching at the same poling condition, the increases in the d_{33} and k_p values could be explained by the increased domain mobility.

The improvement in the d_{33} value in the many studies can be explained by the following thermodynamic theory of the ferroelectric's equation:[34,88,98]

$$d_{33} = 2\varepsilon_{33}{}^{T} Q_{11} P_r \quad (8)$$

where $\varepsilon_{33}{}^{T}$ represents the dielectric constant of the material, P_r is the remnant polarization, and Q_{11} represents the electrostrictive coefficient, which is constant for perovskite materials. This equation demonstrates that the d_{33} is proportional to the P_r value, which matches the data of the current study. Furthermore, for the 8 h annealed ceramic, the P_r increased from 30.02 μC cm^{-2} to 35.85 μC cm^{-2} and E_c slightly dropped from 42.98 kV cm^{-1} to 42.58 kV cm^{-1} (see Table 3), thus resulting in a significant improvement of the d_{33} value for this ceramic.[99] The observed trend in the value of the d_{33} is consistent with the value of the k_p (see Fig. 10).[7,100–103] Maqbool *et al.*[104] also found that the d_{33} and k_p increased when the $SrZrO_3$ (SZ) concentration that was doped in BNT ceramics increased. The significant increase found in d_{33} and k_p at SZ4 was related to a large P_r and a lower E_c because a lower E_c allowed the ceramics to be more easily poled, while a high P_r and P_m favored piezoelectricity. Furthermore, several previous studies proposed that the dielectric constant, piezoelectric constant, and k_p followed a similar trend.[105,106] The improvement of d_{33} and k_p values in the current study is also related to the ferroelectric properties (improve the P_r, P_m, and low E_c), the grain size effect, the MPB, heterogeneous in composition (decrease in the chemical heterogeneity), and also accompanied by the improvement of density, where the trends of d_{33} and k_p values can be matched with the trend of density value (see Tables 1 and 3).

3.8 Energy harvesting behavior

Piezoelectric materials are now attractive for the development of energy harvesting applications. In this current experiment, the energy harvesting properties of the ceramics were investigated. The piezoelectric voltage constant (g_{33}) is one of the important parameters for energy harvesting applications. It has been suggested that the sample with a higher piezoelectric charge constant should generate a higher voltage,[107,108] thus reflecting the quantity of electrical energy produced by the pressure being applied. The g_{33} value can be determined by the following relation:[107–111]

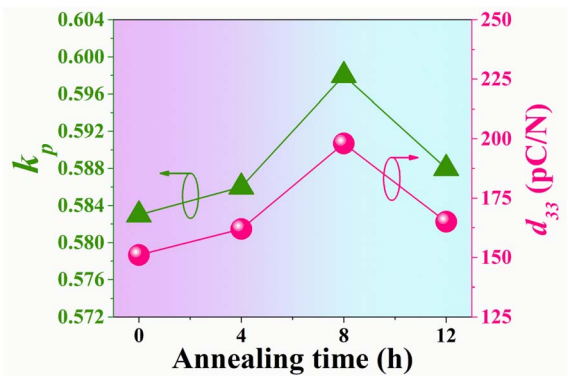

Fig. 10 Plots of the k_p and d_{33} values of the BNKT/0.01ZnO ceramics annealed at 950 °C with different annealing times.

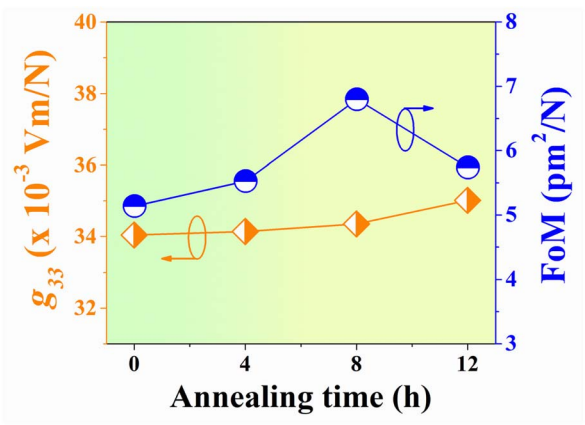

Fig. 11 Plots of the g_{33} and FoM values of the BNKT/0.01ZnO ceramics annealed at 950 °C with different annealing times.

Table 4 Comparison of the d_{33}, g_{33}, and FoM values of the BNKT/0.01ZnO ceramics annealed at 950 °C for 8 h with other lead and lead-free ceramics

System	d_{33} (pC N^{-1})	g_{33} (10^{-3} Vm N^{-1})	FoM (pm^2 N^{-1})	Ref.
BNKT/0.01ZnO (annealed at 950 °C/8 h)	198	34.35	6.80	This work
(BNT–6BT) + 0.1 mol% Al_2O_3	205	31.00	6.36	98
$Ba(Zr_{0.04}Ti_{0.96})O_3$	268	19.11	5.12	107
$Ba(Zr_{0.04}Ti_{0.96})O_3$ + 1 mol% CuO	302	20.64	6.23	107
PZT-70 vol% P(VDF-CTFE)	92	—	6.44	108
0.55BZT–0.45BCT (sintered 1475 °C)	341	16.00	5.46	109
$0.99KNLN_{0.97-x}ST_x - 0.01CZ$ ($x = 0.03$)	225	28.69	6.46	111
$Ba(Zr_{0.07}Ti_{0.93})O_3$ + 2 wt% B_2O_3	291	21.00	6.11	114
(BZT–BCT)-(epoxy-CCTO)	16	—	4.25	115
PZT bulk	556	0.011	6.12	116
PZT micro-pillar	91	0.021	1.91	116
80PZT-PVDF composites (0–3 connectivity)	54	33.95	1.83	117
$0.2(PbMg_{1/3}Nb_{2/3}O_3)$–$0.8(PbZr_{0.475}Ti_{0.525}O_3)$ (bulk-type 1 layer)	241	10.89	2.62	118
0.97[0.995BNKT-0.005LN]-0.03BNdT ceramics	258	14.71	3.80	119
$0.92(Bi_{0.5}Na_{0.5})TiO_3$–$0.08(Ba_{0.5}Sr_{0.5})TiO_3$	118	—	2.85	120

$$g_{33} = \frac{d_{33}}{\varepsilon_r \varepsilon_0} \quad (9)$$

where ε_r is the dielectric constant of the piezoelectric material, ε_0 is the dielectric constant in a vacuum (8.854×10^{-12} F m^{-1}),[112] and d_{33} is the piezoelectric charge constant. From this equation, the generated voltage of the piezoelectric energy harvester depends on the piezoelectric coefficient and dielectric constant of the piezoelectric ceramic. Therefore, the more the piezoelectric charge constant increases, the more the generated voltage also increases.[107] A plot of the g_{33} value of the BNKT/0.01ZnO ceramics at different annealing times is shown in Fig. 11. The g_{33} increased with increasing annealing time, and the highest g_{33} of 35.01×10^{-3} Vm N^{-1} was observed for the 12 h annealed ceramic. The improvement of the g_{33} value for this ceramic is due to the increase of the d_{33}, and the lowering of the ε_r value. This result is consistent with the work done by Choi *et al.*[108]

In this study the energy harvesting performance figure of merit which relates to the g_{33} and d_{33} parameters, was evaluated.[111] In the present investigation, the figure of merit (FoM) parameter was evaluated based on the following equation:[108,109]

$$\text{FoM (pm}^2\text{ N}^{-1}) = d_{33} \times g_{33} \quad (10)$$

where d_{33} is the piezoelectric charge constant, and g_{33} is the piezoelectric voltage constant of the device, respectively. Normally, a piezoelectric material with a high FoM value will produce a large amount of power when utilized for energy harvesting.[113] For the present study, the highest FoM of 6.80 pm^2 N^{-1} was observed for the 8 h annealed ceramic, which was ~32% higher than that of the un-annealed ceramic (see Fig. 11 and Table 3). This improvement is due to the improvements in the d_{33} and g_{33} values for this composition. The results of a comparison of the FoM value for this study with the results of other earlier research studies for different piezoelectric lead-free ceramics are represented in Table 4.[98,107–109,111,114–120] The g_{33} and FoM values for the current experiment are considerably high when compared with other lead free piezoelectric ceramics.

Based on the obtained results, the suitable annealing conditions provided the ceramics with excellence and acceptability for all electrical properties. In this study, the optimum annealing time for the enhancement of dielectric, piezoelectric, and energy harvesting performances of the BNKT/0.01ZnO ceramics was found to be 8 h dwell time.

4 Conclusions

In summary, the effect of thermal annealing time on phase formation, microstructure, dielectric, phase transition, ferroelectric, piezoelectric, and energy harvesting properties of the BNKT/0.01ZnO ceramic prepared by a solid-state reaction technique was investigated. The ceramics which were annealed at 950 °C with different annealing times, exhibited the MPB structure where the rhombohedral and tetragonal phases coexisted, as confirmed by the XRD and Raman measurements. The annealing time made a slight change in the phase transition temperatures, also including the T_d. However, it had significant positive effects on the dielectric, ferroelectric, piezoelectric, and energy harvesting properties of the BNKT/0.01ZnO ceramics, where the optimal annealing time for the current investigation was 8 h.

Author contributions

Pharatree Jaita: writing-original draft preparation. Kamonporn Saenkam: methodology-sample preparation. Gobwute Rujijanagul: conceptualization improve the manuscript and supervisions.

Conflicts of interest

There are no conflicts to declare.

Acknowledgements

This project is funded by National Research Council of Thailand (NRCT) (NRCT5-RSA63004, NRCT5-RSA63004-03) and partially

supported by Chiang Mai University, Research Center in Physics, Astronomy, Materials Sciences Research Center, Global Partnership Project (B16F640001), and CMU Junior Research Fellowship Program (JRCMU2565_058). Office of Research Administration, Department of Physics and Materials Science, Faculty of Science, and Science and Technology Research Institute, Chiang Mai University are also acknowledged.

References

1 J. Feng, R. Huang, Z. Liang, Z. Du, Y. Dai, J. Wu and H. T. Lin, The effect of B site doping of Nb^{5+} and aging process on the properties of BNKT-BT lead-free piezoelectric ceramics, *Ceram. Int.*, 2022, **48**, 2355–2361.

2 J. Camargo, S. Osinaga, M. Febbo, S. P. Machado, F. R. Marcos, L. Ramajo and M. Castro, Piezoelectric and structural properties of bismuth sodium potassium titanate lead-free ceramics for energy harvesting, *J. Mater. Sci.: Mater. Electron.*, 2021, **32**, 19117–19125.

3 A. Chauhan, S. Patel, G. Vats and R. Vaish, Enhanced thermal energy harvesting using Li, K-Doped $Bi_{0.5}Na_{0.5}TiO_3$ lead-free ferroelectric ceramics, *Energy Technol.*, 2014, **2**, 205–209.

4 S. Zhao, H. Wu and Q. Sun, Study on PSN-PZN-PZT quaternary piezoelectric ceramics near the morphotropic phase boundary, *Mater. Sci. Eng., B*, 2005, **123**, 203–210.

5 N. P. M. J. Raj, G. Khandelwal and S. J. Kim, 0.8BNT-0.2BKT ferroelectric-based multimode energy harvester for self-powered body motion sensors, *Nanomater. Energy*, 2021, **83**, 105848.

6 X. Qiao, D. Wu, F. Zhang, M. Niu, B. Chen, X. Zhao, P. Liang, L. Wei, X. Chao and Z. Yang, Enhanced energy density and thermal stability in relaxor ferroelectric $Bi_{0.5}Na_{0.5}TiO_3$-$Sr_{0.7}Bi_{0.2}TiO_3$ ceramics, *J. Eur. Ceram. Soc.*, 2019, **39**, 4778–4784.

7 A. Ullah, C. W. Ahn and I. W. Kim, Dielectric, piezoelectric properties and field-induced large strain of $Bi(Zn_{0.5}Ti_{0.5})O_3$-modified morphotropic phase boundary $Bi_{0.5}(Na_{0.82}K_{0.18})_{0.5}TiO_3$ piezoelectric ceramics, *Jpn. J. Appl. Phys.*, 2012, **51**, 09MD07.

8 Y. Zhang, X. Liu, G. Wang, Y. Li, S. Zhang, D. Wang and H. Sun, Enhanced mechanical energy harvesting capability in sodium bismuth titanate based lead-free piezoelectric, *J. Alloys Compd.*, 2020, **825**, 154020.

9 Z. Yang, B. Liu, L. Wei and Y. Hou, Structure and electrical properties of (1-*x*)$Bi_{0.5}Na_{0.5}TiO_3$-*x*$Bi_{0.5}K_{0.5}TiO_3$ ceramics near morphotropic phase boundary, *Mater. Res. Bull.*, 2008, **43**, 81–89.

10 A. Sasaki, T. Chiba, Y. Mamiya and E. Otsuki, Dielectric and piezoelectric properties of $(Bi_{0.5}Na_{0.5})TiO_3$-$(Bi_{0.5}K_{0.5})TiO_3$ systems, *Jpn. J. Appl. Phys.*, 1999, **38**, 5564–5567.

11 K. Yoshii, Y. Hiruma, H. Nagata and T. Takenaka, Electrical properties and depolarization temperature of $(Bi_{1/2}Na_{1/2})TiO_3$-$(Bi_{1/2}K_{1/2})TiO_3$ lead-free piezoelectric ceramics, *Jpn. J. Appl. Phys.*, 2006, **45**, 4493–4496.

12 P. Jaita, A. Watcharapasorn, N. Kumar, S. Jiansirisomboon and D. P. Cann, Lead-free $(Ba_{0.70}Sr_{0.30})TiO_3$-modified $Bi_{0.5}(Na_{0.80}K_{0.20})_{0.5}TiO_3$ ceramics with large electric field-induced strains, *J. Am. Ceram. Soc.*, 2016, **99**, 1615–1624.

13 X. Ren, H. Fan, Y. Zhao and Z. Liu, Flexible lead-free $BiFeO_3$/PDMS-based nanogenerator as piezoelectric energy harvester, *ACS Appl. Mater. Interfaces*, 2016, **8**, 26190–26197.

14 M. M. Alam, S. K. Ghosh, A. Sultana and D. Mandal, Lead-free $ZnSnO_3$/MWCNTs-based selfpoled flexible hybrid nanogenerator for piezoelectric power generation, *Nanotechnology*, 2015, **26**, 165403.

15 M. Promsawat, A. Watcharapasorn, H. N. Tailor, S. Jiansirisomboon and Z. G. Ye, Enhanced dielectric, ferroelectric, and electrostrictive properties of $Pb(Mg_{1/3}Nb_{2/3})_{0.9}Ti_{0.1}O_3$ ceramics by ZnO modification, *J. Appl. Phys.*, 2013, **113**, 204101.

16 Y. C. Lee, T. K. Lee and J. H. Jan, Piezoelectric properties and microstructures of ZnO-doped $Bi_{0.5}Na_{0.5}TiO_3$ ceramics, *J. Eur. Ceram. Soc.*, 2011, **31**, 3145–3152.

17 F. R. Marcos, J. J. Romero, M. G. N. Rojero and J. F. Fernandez, Effect of ZnO on the structure, microstructure and electrical properties of KNN-modified piezoceramics, *J. Eur. Ceram. Soc.*, 2009, **29**, 3045–3052.

18 J. Zhang, Z. Pan, F. F. Guo, W. C. Liu, H. Ning, Y. B. Chen, M. H. Lu, B. Yang, J. Chen, S. T. Zhang, X. Xing, J. Rödel, W. Cao and Y. F. Chen, Semiconductor/relaxor 0-3 type composites without thermal depolarization in $Bi_{0.5}Na_{0.5}TiO_3$-based lead-free piezoceramics, *Nat. Commun.*, 2015, **6**, 6615.

19 S. Manotham, P. Jaita, P. Butnoi, N. Lertcumfu and G. Rujijanagul, Improvements of depolarization temperature, piezoelectric and energy harvesting properties of BNT-based ceramics by doping an interstitial dopant, *J. Alloys Compd.*, 2022, **897**, 163021.

20 X. Zhang, G. Jiang, D. Liu, B. Yang and W. Cao, Improved depolarization behavior and electric properties in $(Bi_{0.5}Na_{0.5})TiO_3$-based piezoelectric composites, *J. Alloys Compd.*, 2018, **769**, 660–668.

21 W. P. Cao, W. L. Li, Y. Feng, D. Xu, W. Wang, Y. F. Hou, T. D. Zhang and W. D. Fei, Enhanced depolarization temperature in 0.90NBT-0.05KBT-0.05BT ceramics induced by BT nanowires, *J. Phys. Chem. Solids*, 2015, **78**, 41–45.

22 L. Wang, T. K. Song, S. C. Lee, J. H. Cho, Y. S. Sung, M. H. Kim and K. S. Choi, Dielectric and piezoelectric properties of Li-substituted lead-free $(Bi_{0.5}Na_{0.5})TiO_3$-$(Bi_{0.5}K_{0.5})TiO_3$-$BaTiO_3$ ceramics, *Curr. Appl. Phys.*, 2010, **10**, 1059–1061.

23 Y. Watanabe, Y. Hiruma, H. Nagata and T. Takenaka, Phase transition temperatures and electrical properties of divalent ions (Ca^{2+}, Sr^{2+} and Ba^{2+}) substituted $(Bi_{1/2}Na_{1/2})TiO_3$ ceramics, *Ceram. Int.*, 2008, **34**, 761–764.

24 A. Maqbool, A. Hussain, J. U. Rahman, T. K. Song, W. J. Kim, J. Lee and M. H. Kim, Enhanced electric field-induced strain and ferroelectric behavior of $(Bi_{0.5}Na_{0.5})TiO_3$-$BaTiO_3$-$SrZrO_3$ lead-free ceramics, *Ceram. Int.*, 2014, **40**, 11905–11914.

25 Q. Xu, Y. H. Huang, M. Chen, W. Chen, B. H. Kim and B. K. Ahn, Effect of bismuth deficiency on structure and

electrical properties of $(Na_{0.5}Bi_{0.5})_{0.93}Ba_{0.07}TiO_3$ ceramics, *J. Phys. Chem. Solids*, 2008, **69**, 1996–2003.

26 X. S. Qiao, X. M. Chen, H. L. Lian, W. T. Chen, J. P. Zhou and P. Liu, Microstructure and electrical properties of nonstoichiometric $0.94(Na_{0.5}Bi_{0.5+x})TiO_3$-$0.06BaTiO_3$ lead-free ceramics, *J. Am. Ceram. Soc.*, 2016, **99**, 198–205.

27 J. Yin, Y. Wang, Y. Zhang, B. Wu and J. Wu, Thermal depolarization regulation by oxides selection in lead-free BNT/oxides piezoelectric composites, *Acta Mater.*, 2018, **158**, 269–277.

28 W. Bai, L. Wang, P. Zheng, F. Wen, J. Zhai and Z. Ji, Pairing high piezoelectric properties and enhanced thermal stability in grain-oriented BNT-based lead-free piezoceramics, *Ceram. Int.*, 2018, **44**, 11402–11409.

29 M. Ghasemifard, M. Daneshvar and M. Ghamari, The Effects of annealing process on dielectric and piezoelectric properties of BMT-base lead-free ceramics, *World J. Nano Sci. Eng.*, 2013, **3**, 100–107.

30 G. Rujijanagul, N. Vittayakorn and S. Nabunmee, Effect of annealing time on electrical and mechanical properties of $0.7(Pb(Zr_{1/2}Ti_{1/2})O_3)$-$0.3(Pb(Zn_{1/2}Nb_{2/3})O_3)$ ceramics, *Ferroelectrics*, 2009, **384**, 68–72.

31 J. Xu, Q. Li, L. Yang, W. Zeng, C. Zhou, C. Yuan, G. Chen and G. Rao, Effects of thermal and electrical histories on structure and dielectric behaviors of $(Li_{0.5}Nd_{0.5})^{2+}$-modified $(Bi_{0.5}Na_{0.5})TiO_3$-$BaTiO_3$ ceramics, *J. Materiomics*, 2017, **3**, 121–129.

32 K. Wang, B. P. Zhang, J. F. Li and L. M. Zhang, Lead-free $Na_{0.5}K_{0.5}NbO_3$ piezoelectric ceramics fabricated by spark plasma sintering: Annealing effect on electrical properties, *J. Electroceram.*, 2008, **21**, 251–254.

33 S. Hajra, S. Sahoo, R. Das and R. N. P. Choudhary, Structural, dielectric and impedance characteristics of $(Bi_{0.5}Na_{0.5})TiO_3$-$BaTiO_3$ electronic system, *J. Alloys Compd.*, 2018, **750**, 507–514.

34 A. Ullah, C. W. Ahn, A. Hussain, I. W. Kim, H. I. Hwang and N. K. Cho, Structural transition and large electric field-induced strain in $BiAlO_3$-modified $Bi_{0.5}(Na_{0.8}K_{0.2})_{0.5}TiO_3$ lead-free piezoelectric ceramics, *Solid State Commun.*, 2010, **150**, 1145–1149.

35 K. N. Pham, A. Hussain, C. W. Ahn, I. W. Kim, S. J. Jeong and J. S. Lee, Giant strain in Nb doped $Bi_{0.5}(Na_{0.82}K_{0.18})_{0.5}TiO_3$ lead-free electromechanical ceramics, *Mater. Lett.*, 2010, **64**, 2219–2222.

36 B. D. Cullity, *Elements of X-ray Diffraction*. Addison-Wesley Publishing, Philippines, 1978.

37 R. Rafique, K. N. Tonny, A. Sharmin and Z. H. Mahmood, Study on the effect of varying film thickness on the transparent conductive nature of aluminum doped zinc oxide deposited by dip coating, *Mater. Focus*, 2018, **7**, 1–7.

38 A. Hosseinmardi, N. Shojaee, M. K. Rad and T. Ebadzadeh, A study on the photoluminescence properties of electrospray deposited amorphous and crystalline nanostructured ZnO thin films, *Ceram. Int.*, 2012, **38**, 1975–1980.

39 M. J. Lee, T. I. Lee, J. Lim, J. Bang, W. Lee, T. Lee and J. M. Myoung, Effect of the deposition temperature and a hydrogen post-annealing treatment on the structural, electrical, and optical properties of Ga-doped ZnO films, *Electron. Mater. Lett.*, 2009, **5**, 127–133.

40 A. Zaier, A. Meftah, A. Y. Jaber, A. A. Abdelaziz and M. S. Aida, Annealing effects on the structural, electrical and optical properties of ZnO thin films prepared by thermal evaporation technique, *J. King Saud Univ., Sci.*, 2015, **27**, 356–360.

41 A. Gahtar, A. Benali, S. Benramache and C. Zaouche, Effect of annealing time on the structural, morphological, optical and electrical properties of NiS thin films, *Chalcogenide Lett.*, 2022, **19**, 103–116.

42 K. A. Razak, C. J. Yip and S. Sreekantan, Synthesis of $(Bi_{0.5}Na_{0.5})TiO_3$ (BNT) and Pr doped BNT using the soft combustion technique and its properties, *J. Alloys Compd.*, 2011, **509**, 2936–2941.

43 N. D. Co, L. V. Cuong, B. D. Tu, P. D. Thang, L. X. Dien, V. N. Hung and N. D. Quan, Effect of crystallization temperature on energy-storage density and efficiency of lead-free $Bi_{0.5}(Na_{0.8}K_{0.2})_{0.5}TiO_3$ thin films prepared by sol-gel method, *J. Sci.: Adv. Mater. Devices*, 2019, **4**, 370–375.

44 S. Wada, K. Yamato, P. Pulpan, N. Kumada, B. Y. Lee, T. Iijima, C. Moriyoshi and Y. Kuroiwa, Piezoelectric properties of high Curie temperature barium titanate-bismuth perovskite-type oxide system ceramics, *J. Appl. Phys.*, 2010, **108**, 094114.

45 S. Wada, K. Yamato, P. Pulpan, N. Kumada, B. Y. Lee, T. Iijima, C. Moriyoshi and Y. Kuroiwa, Preparation of barium titanate-bismuth magnesium titanate ceramics with high Curie temperature and their piezoelectric properties, *J. Ceram. Soc. Jpn.*, 2010, **118**, 683–687.

46 M. Difeo, S. Osinaga, M. Febbo, S. P. Machado, M. Castro and L. Ramajo, Influence of the $(Bi_{0.5}Na_{0.5})TiO_3$-$BaTiO_3$ lead-free piezoceramic geometries on the power generation of energy harvesting devices, *Ceram. Int.*, 2021, **47**, 10696–10704.

47 D. Rout, K. S. Moon, S. J. L. Kang and I. W. Kim, Dielectric and Raman scattering studies of phase transitions in the $(100\text{-}x)Na_{0.5}Bi_{0.5}TiO_3$-$xSrTiO_3$ system, *J. Appl. Phys.*, 2010, **108**, 084102.

48 S. Prasertpalichat, T. Siritanon, N. Nuntawong and D. P. Cann, Structural characterization of A-site nonstoichiometric $(1\text{-}x)Bi_{0.5}Na_{0.5}TiO_3$-$xBaTiO_3$ ceramics, *J. Mater. Sci.*, 2019, **54**, 1162–1170.

49 J. Wang, C. Zhou, Q. Li, W. Zeng, J. Xu, G. Chen, C. Yuan and G. Rao, Dual relaxation behaviors and large electrostrictive properties of $Bi_{0.5}Na_{0.5}TiO_3$-$Sr_{0.85}Bi_{0.1}TiO_3$ ceramics, *J. Mater. Sci.*, 2018, **53**, 8844–8854.

50 M. Zhong, Q. Feng, C. Yuan, X. Liu, B. Zhu, L. Meng, C. Zhou, J. Xu, J. Wang and G. Rao, Photocurrent density and electrical properties of $Bi_{0.5}Na_{0.5}TiO_3$-$BaNi_{0.5}Nb_{0.5}O_3$ ceramics, *J. Adv. Ceram.*, 2021, **10**, 1119–1128.

51 J. Hao, B. Shen, J. Zhai, C. Liu, X. Li and X. Gao, Large strain response in $0.99(Bi_{0.5}Na_{0.4}K_{0.1})TiO_3$-$0.01(K_xNa_{1-x})NbO_3$ lead-free ceramics induced by the change of K/Na ratio in $(K_xNa_{1\text{-}x})NbO_3$, *J. Am. Ceram. Soc.*, 2013, **96**, 3133–3140.

52 P. Jarupoom and G. Rujijanagul, Improvement in piezoelectric strain of annealed $Ba(Zr_{0.07}Ti_{0.93})O_3$ based ceramics, *J. Appl. Phys.*, 2013, **114**, 027018.

53 S. Eitssayeam, P. Jarupoom and G. Rujijanagul, High dielectric and piezoelectric properties observed in annealed $Pb_{0.88}Sr_{0.12}Zr_{0.54}Ti_{0.44}Sb_{0.02}O_3$ ceramics, *Ferroelectrics*, 2013, **451**, 48–53.

54 M. F. Mat, Y. H. P. Manurung, N. Muhammad, S. N. S. Ahmad, M. Graf and M. S. Sulaiman, Variable analysis for grain size prediction of austenitic stainless steel SS316l using heat treatment, *J. Appl. Sci.*, 2020, **20**, 91–96.

55 Y. Hiruma, H. Nagata and T. Takenaka, Grain-size effect on electrical properties of $(Bi_{1/2}K_{1/2})TiO_3$ ceramics, *Jpn. J. Appl. Phys.*, 2007, **46**, 1081–1084.

56 X. Zhou, G. Xue, H. Luo, C. R. Bowen and D. Zhang, Phase structure and properties of sodium bismuth titanate lead-free piezoelectric ceramics, *Prog. Mater. Sci.*, 2021, **122**, 100836.

57 Q. Li, L. Ning, C. Wang and H. Fan, Gaint electric field-induced strain and ferroelectric behavior of $Bi_{0.5}Na_{0.4}K_{0.1}TiO_3$-$Na_{1-x}Li_xNbO_3$ lead-free ceramics, *Mater. Sci. Eng., B*, 2021, **263**, 114819.

58 M. Habib, M. Munir, S. A. Khan, T. K. Song, M. H. Kim, M. J. Iqbal, I. Qazi and A. Hussain, Evaluation of high strain response in lead-free BNBTFS-*x*Nb ceramics by structure and ferroelectric characterizations, *J. Phys. Chem. Solids*, 2020, **138**, 109230.

59 F. Xia and X. Yao, Postsintering annealing induced extrinsic dielectric and piezoelectric responses in lead-zinc-niobate-based ferroelectric ceramics, *J. Appl. Phys.*, 2002, **92**, 2709–2716.

60 V. R. Mudinepalli, L. Feng, W. C. Lin and B. S. Murty, Effect of grain size on dielectric and ferroelectric properties of nanostructured $Ba_{0.8}Sr_{0.2}TiO_3$ ceramics, *J. Adv. Ceram.*, 2015, **4**, 46–53.

61 Z. Zhao, V. Buscaglia, M. Viviani, M. T. Buscaglia, L. Mitoseriu, A. Testino, M. Nygren, M. Johnsson and P. Nanni, Grain-size effects on the ferroelectric behavior of dense nanocrystalline $BaTiO_3$ ceramics, *Phys. Rev. B: Condens. Matter Mater. Phys.*, 2004, **70**, 024107.

62 S. K. Gupta, R. M. Quade, B. Gibbons, P. Mardilovich and D. P. Cann, Electric field-induced strain in $Sr(Hf_{0.5}Zr_{0.5})O_3$-modified $Bi_{0.5}(Na_{0.8}K_{0.2})_{0.5}TiO_3$ piezoelectric ceramics, *J. Appl. Phys.*, 2020, **127**, 074104.

63 A. Bhalla, R. Guo, L. Cross, G. Burns, F. Dacol and R. R. Neurgaonkar, Measurements of strain and the optical indices in the ferroelectric $Ba_{0.4}Sr_{0.6}Nb_2O_6$: Polarization effects, *Phys. Rev. B: Condens. Matter Mater. Phys.*, 1987, **36**, 2030–2035.

64 K. Uchino, S. Nomura, L. E. Cross, R. E. Newnham and S. J. Jang, Electrostrictive effect in perovskites and its transducer applications, *J. Mater. Sci.*, 1981, **16**, 569–578.

65 Z. Yang, H. Du, L. Jin, Q. Hu, H. Wang, Y. Li, J. Wang, F. Gao and S. Qu, Realizing high comprehensive energy storage performance in lead-free bulk ceramics *via* designing an unmatched temperature range, *J. Mater. Chem. A*, 2019, **7**, 27256.

66 R. Kang, Z. Wang, X. Lou, W. Liu, P. Shi, X. Zhu, X. Guo, S. Li, H. Sun, L. Zhang and Q. Sun, Energy storage performance of $Bi_{0.5}Na_{0.5}TiO_3$-based relaxor ferroelectric ceramics with superior temperature stability under low electric fields, *Chem. Eng. J.*, 2021, **410**, 128376.

67 S. B. Li, C. B. Wang, L. Li, Q. Shen and L. M. Zhang, Effect of annealing temperature on structural and electrical properties of BCZT ceramics prepared by plasma activated sintering, *J. Alloys Compd.*, 2018, **730**, 182–190.

68 K. Uchino and S. Nomura, Critical exponents of the dielectric constants in diffused-phase-transition crystals, *Ferroelectr., Lett.*, 1982, **44**, 55–61.

69 Q. Hu, Y. Tian, Q. Zhu, J. Bian, L. Jin, H. Du, D. O. Alikin, V. Y. Shur, Y. Feng, Z. Xu and X. Wei, Achieve ultrahigh energy storage performance in $BaTiO_3$-$Bi(Mg_{1/2}Ti_{1/2})O_3$ relaxor ferroelectric ceramics *via* nano-scale polarization mismatch and reconstruction, *Nano Energy*, 2020, **67**, 104264.

70 J. Li, D. Zhang, S. Qin, T. Li, M. Wu, D. Wang, Y. Bai and X. Lou, Large room-temperature electrocaloric effect in lead-free $BaHf_xTi_{1-x}O_3$ ceramics under low electric field, *Acta Mater.*, 2016, **115**, 58–67.

71 E. M. Anton, W. Jo, D. Damjanovic and J. Rodel, Determination of depolarization temperature of $(Bi_{1/2}Na_{1/2})TiO_3$-based lead-free piezoceramics, *J. Appl. Phys.*, 2011, **110**, 094108.

72 Y. J. Dai and X. W. Zhang, An approach to improve the piezoelectric property of $(Bi_{0.5}Na_{0.5})TiO_3$-$(Bi_{0.5}K_{0.5})TiO_3$-$BaTiO_3$ lead-free ceramics, *Int. J. Appl. Ceram. Technol.*, 2011, **8**, 423–429.

73 J. J. Wang, F. F. Guo, B. Yang, S. T. Zhang, L. M. Zheng, F. M. Wu and W. W. Cao, Electrical properties of $0.94Bi_{0.5}Na_{0.5}TiO_3$-$0.06Ba(Zr_{0.055}Ti_{0.945})O_3$ lead-free ceramics with high thermal stability, *J. Mater. Sci.: Mater. Electron.*, 2018, **29**, 2357–2362.

74 J. Wang, C. Zhou, Q. Li, L. Yang, J. Xu, G. Chen, C. Yuan and G. Rao, Simultaneously enhanced piezoelectric properties and depolarization temperature in calcium doped $BiFeO_3$-$BaTiO_3$ ceramics, *J. Alloys Compd.*, 2018, **748**, 758–765.

75 A. Mahajan, H. Zhang, J. Wu, E. V. Ramana, M. J. Reece and H. Yan, Effect of phase transitions on thermal depoling in lead-free $0.94Bi_{0.5}Na_{0.5}TiO_3$-$0.06BaTiO_3$ based piezoelectrics, *J. Phys. Chem. C*, 2017, **121**, 5709–5718.

76 L. Li, M. Zhu, K. Zhou, Q. Wei, M. Zheng and Y. Hou, Delayed thermal depolarization of $Bi_{0.5}Na_{0.5}TiO_3$-$BaTiO_3$ by doping acceptor Zn^{2+} with large ionic polarizability, *J. Appl. Phys.*, 2017, **122**, 204104.

77 M. Davies, E. Aksel and J. L. Jones, Enhanced high-temperature piezoelectric coefficients and thermal stability of Fe-and Mn-substituted $Na_{0.5}Bi_{0.5}TiO_3$ ceramics, *J. Am. Ceram. Soc.*, 2011, **94**, 1314–1316.

78 L. M. Riemer, K. V. Lalitha, X. Jiang, N. Liu, C. Dietz, R. W. Stark, P. B. Groszewicz, G. Buntkowsky, J. Chen, S. T. Zhang, J. Rödel and J. Koruza, Stress-induced phase

transition in lead-free relaxor ferroelectric composites, *Acta Mater.*, 2017, **136**, 271–280.

79 N. W. Thomas, A new framework for understanding relaxor ferroelectrics, *J. Phys. Chem. Solids*, 1990, **51**, 1419–1431.

80 Z. Yang, Y. Hou, B. Liu and L. Wei, Structure and electrical properties of Nd_2O_3-doped $0.82Bi_{0.5}Na_{0.5}TiO_3$-$0.18Bi_{0.5}K_{0.5}TiO_3$ ceramics, *Ceram. Int.*, 2009, **35**, 1423–1427.

81 N. Y. Quyet, L. H. Bac and D. D. Dung, Effect of Li_2CO_3 addition on the structural, optical, ferroelectric, and electric-field-induced strain of lead-free BNKT-based ceramics, *J. Phys. Chem. Solids*, 2015, **85**, 148–154.

82 H. Nagata, Y. Takagi, Y. Yoneda and T. Takenaka, Correlation between depolarization temperature and lattice distortion in quenched $(Bi_{1/2}Na_{1/2})TiO_3$-based ceramics, *Appl. Phys. Express*, 2020, **13**, 061002.

83 D. K. Khatua, A. Mishra, N. Kumar, G. D. Adhikary, U. Shankar, B. Majumdar and R. Ranjan, A coupled microstructural-structural mechanism governing thermal depolarization delay in $Na_{0.5}Bi_{0.5}TiO_3$-based piezoelectrics, *Acta Mater.*, 2019, **179**, 49–60.

84 L. Jin, F. Li and S. Zhang, Decoding the fingerprint of ferroelectric loops: comprehension of the material properties and structures, *J. Am. Ceram. Soc.*, 2014, **97**, 1–27.

85 N. Vittayakorn, G. Rujijanagul and D. P. Cann, The improvement in dielectric and ferroelectric performance of PZT-PZN ceramics by thermal treatment, *Curr. Appl. Phys.*, 2007, **7**, 582–585.

86 G. Dong, H. Fan, J. Shi and M. Li, Composition- and temperature-dependent large strain in $(1-x)(0.8Bi_{0.5}Na_{0.5}TiO_3$-$0.2Bi_{0.5}K_{0.5}TiO_3)$-$xNaNbO_3$ ceramics, *J. Am. Ceram. Soc.*, 2015, **98**, 1150–1155.

87 Y. Huan, X. Wang, J. Fang and L. Li, Grain size effect on piezoelectric and ferroelectric properties of $BaTiO_3$ ceramics, *J. Eur. Ceram. Soc.*, 2014, **34**, 1445–1448.

88 J. Hao, W. Bai, W. Li and J. Zhai, Correlation between the microstructure and electrical properties in high-performance $(Ba_{0.85}Ca_{0.15})(Zr_{0.1}Ti_{0.9})O_3$ lead-free piezoelectric ceramics, *J. Am. Ceram. Soc.*, 2012, **95**, 1998–2006.

89 G. H. Haertling and W. J. Zimmer, An analysis of hot-pressing parameters for lead zirconate lead titanate ceramics containing two atom percent bismuth, *Am. Ceram. Soc. Bull.*, 1966, **45**, 1084–1089.

90 P. Jarupoom, T. Tunkasiri, K. Pengpat, S. Eitssayeam and G. Rujijanagul, Effects of annealing time on ferroelectric and piezoelectric properties of B_2O_3 doped $Ba(Zr_{0.07}Ti_{0.93})O_3$ ceramics, *Ferroelectrics*, 2011, **415**, 88–93.

91 B. M. Jin, J. Kim and S. C. Kim, Effects of grain size on the electrical properties of $PbZr_{0.52}Ti_{0.48}O_3$ ceramics, *Appl. Phys. A*, 1997, **65**, 53–56.

92 G. Ray, N. Sinha and B. Kumar, Environment friendly novel piezoelectric $0.94[Na_{0.8}K_{0.2}NbO_3]$-$0.06LiNbO_3$ ternary ceramic for high temperature dielectric and ferroelectric applications, *Mater. Chem. Phys.*, 2013, **142**, 619–625.

93 C. C. Jin, F. F. Wang, Q. R. Yao, Y. X. Tang, T. Wang and W. Z. Shi, Ferroelectric, dielectric properties and large strain response in Zr-modified $(Bi_{0.5}Na_{0.5})TiO_3$-$BaTiO_3$ lead-free ceramics, *Ceram. Int.*, 2014, **40**, 6143–6150.

94 Z. T. Li, H. Liu, H. C. Thong, Z. Xu, M. H. Zhang, J. Yin, J. F. Li, K. Wang and J. Chen, Enhanced temperature stability and defect mechanism of BNT-based lead-free piezoceramics investigated by a quenching process, *Adv. Electron. Mater.*, 2019, **5**, 1800756.

95 A. B. Swain, S. D. Kumar, V. Subramanian and P. Murugavel, Influence of external electric field on the physical characteristics of lead free BZT-BCT piezoceramic, *J. Alloys Compd.*, 2019, **787**, 990–995.

96 B. H. Chen, C. L. Huang and L. Wu, Promotion of piezoelectric properties of lead zirconate titanate ceramics with (Zr,Ti) partially replaced by Nb_2O_5, *Solid-State Electron.*, 2004, **48**, 2293–2297.

97 B. S. Kang, D. G. Choi and S. K. Choi, Effects of grain size on pyroelectric and dielectric properties of $Pb_{0.9}La_{0.1}TiO_3$ ceramics, *J. Mater. Sci.: Mater. Electron.*, 1998, **9**, 139–144.

98 P. Jaita, S. Manotham and G. Rujijanagul, Influence of Al_2O_3 nanoparticle doping on depolarization temperature, and electrical and energy harvesting properties of lead-free $0.94(Bi_{0.5}Na_{0.5})TiO_3$-$0.06BaTiO_3$ ceramics, *RSC Adv.*, 2020, **10**, 32078–32087.

99 A. Ullah, C. W. Ahn, K. B. Jang, A. Hussain and I. W. Kim, Phase transition and electrical properties of $BiAlO_3$-modified $(Bi_{0.5}Na_{0.5})TiO_3$ piezoelectric ceramics, *Ferroelectrics*, 2010, **404**, 167–172.

100 K. Yoshii, Y. Hiruma, H. Nagata and T. Takenaka, Electrical properties and depolarization temperature of $(Bi_{1/2}Na_{1/2})TiO_3$-$(Bi_{1/2}K_{1/2})TiO_3$ lead-free piezoelectric ceramics, *Jpn. J. Appl. Phys.*, 2006, **45**, 4493–4496.

101 B. P. Zhang, J. F. Li, K. Wang and H. Zhangy, Compositional dependence of piezoelectric properties in $Na_xK_{1-x}NbO_3$ lead-free ceramics prepared by spark plasma sintering, *J. Am. Ceram. Soc.*, 2006, **89**, 1605–1609.

102 Z. Chen, J. Hu and X. He, Piezoelectric and dielectric properties of $(Na_{0.5}K_{0.5})NbO_3$-$Bi_{0.5}(Na_{0.8}K_{0.2})_{0.5}TiO_3$ lead-free ceramics, *J. Ceram. Soc. Jpn.*, 2008, **116**, 661–663.

103 Z. C. Rong and C. L. Yuan, Dielectric and piezoelectric properties of $Bi_{0.5}(Na_{0.82}K_{0.18})_{0.5}TiO_3$-$LiSbO_3$ lead-free piezoelectric ceramics, *Bull. Mater. Sci.*, 2011, **34**, 933–936.

104 A. Maqbool, J. Rahman, A. Hussain, J. K. Park, T. G. Park, J. S. Song and M. H. Kim, Structure and temperature dependent electrical properties of lead-free $Bi_{0.5}Na_{0.5}TiO_3$-$SrZrO_3$ ceramics, *IOP Conf. Ser.: Mater. Sci. Eng.*, 2014, **60**, 012047.

105 K. Ohbayashi, T. Matsuoka, K. Kitamura, H. Yamada, T. Hishida and M. Yamazaki, Lead-free piezoelectric $(K,Na)NbO_3$-based ceramic with planar-mode coupling coefficient comparable to that of conventional lead zirconate titanate, *Jpn. J. Appl. Phys.*, 2017, **56**, 061501.

106 Y. Yu, J. Wu, T. Zhao, S. Dong, H. Gu and Y. Hu, MnO_2 doped PSN-PZN-PZT piezoelectric ceramics for resonant actuator application, *J. Alloys Compd.*, 2014, **615**, 676–682.

107 D. J. Shin and J. H. Koh, Comparative study on storing energy for $(Ba,Zr)TiO_3$ and CuO-$(Ba,Zr)TiO_3$ ceramics for

piezoelectric energy harvesting applications, *Ceram. Int.*, 2017, **43**, S649–S654.

108 Y. J. Choi, M. J. Yoo, H. W. Kang, H. G. Lee, S. H. Han and S. Nahm, Dielectric and piezoelectric properties of ceramic-polymer composites with 0-3 connectivity type, *J. Electroceram.*, 2013, **30**, 30–35.

109 D. J. Shin, J. Kim and J. H. Koh, Piezoelectric properties of (1-*x*)BZT-*x*BCT system for energy harvesting applications, *J. Eur. Ceram. Soc.*, 2018, **38**, 4395–4403.

110 H. Zhao, Y. Hou, X. Yu, J. Fu, M. Zheng and M. Zhu, A wide temperature insensitive piezoceramics for high temperature energy harvesting, *J. Am. Ceram. Soc.*, 2019, **102**, 5316–5327.

111 B. Liu, P. Li, B. Shen, J. Zhai, Y. Zhang, F. Li and X. Liu, Simultaneously enhanced piezoelectric response and piezoelectric voltage coefficient in textured KNN-based ceramics, *J. Am. Ceram. Soc.*, 2018, **101**, 265–273.

112 U. De, K. R. Sahu and A. De, Ferroelectric materials for high temperature piezoelectric applications, *Solid State Phenom.*, 2015, **232**, 235–278.

113 H. Li, C. Tian and Z. D. Deng, Energy harvesting from low frequency applications using piezoelectric materials, *Appl. Phys. Rev.*, 2014, **1**, 041301.

114 P. Jarupoom, K. Pengpat and G. Rujijanagul, Enhanced piezoelectric properties and lowered sintering temperature of $Ba(Zr_{0.07}Ti_{0.93})O_3$ by B_2O_3 addition, *Curr. Appl. Phys.*, 2010, **10**, 557–560.

115 P. Mishra and P. Kumar, Enhancement of dielectric properties of 0.2[BZT-BCT]-0.8[(1-*x*)epoxy-*x*CCTO] (x = 0.02, 0.04, 0.06, 0.08 & 0.1) composites for embedded capacitor and energy harvesting applications, *J. Alloys Compd.*, 2014, **617**, 899–904.

116 D. J. Shin and J. H. Koh, A micro pattern of fine scale PZT ceramic structures for the energy harvester, Int, *Ferroelectrics*, 2012, **140**, 84–91.

117 P. Gowdhaman, V. Annamalai and O. P. Thakur, Piezo, ferro and dielectric properties of ceramic-polymer composites of 0-3 connectivity, *Ferroelectrics*, 2016, **493**, 120–129.

118 D. J. Shin, W. S. Kang, J. H. Koh, K. H. Cho, C. E. Seo and S. K. Lee, Comparative study between the pillar and bulk-type multilayer structures for piezoelectric energy harvesters, *Phys. Status Solidi A*, 2014, **211**, 1812–1817.

119 P. Wannasut, P. Jaita, M. Promsawat and A. Watcharapasorn, Enhanced electrical properties of new lead-free $0.995Bi_{0.5}(Na_{0.80}K_{0.20})_{0.5}TiO_3$-$0.005LiNbO_3$ ceramics by $(Ba_{0.98}Nd_{0.02})TiO_3$ doping, *J. Asian Ceram. Soc.*, 2021, **9**, 1345–1353.

120 Y. H. Kwon, D. J. Shin and J. H. Koh, (1-*x*)(Bi,Na)TiO_3-*x*(Ba,Sr)TiO_3 lead-free piezoelectric ceramics for piezoelectric energy harvesting, *J. Korean Phys. Soc.*, 2015, **66**, 1067–1071.